

# New Josephson Plasma Modes in Underdoped $\text{YBa}_2\text{Cu}_3\text{O}_{6.6}$ Induced by Parallel Magnetic Field

K. M. Kojima\* and S. Uchida

*Graduate School of Frontier Sciences, University of Tokyo, Hongo 7-3-1, Bunkyo, Tokyo 113-8656, Japan*

Y. Fudamoto and S. Tajima

*Superconductivity Research Laboratory, ISTEK, Shinonome 1-10-13, Koto-ku, Tokyo 135-0062, Japan*

(Dated: )

The  $c$ -axis reflectivity spectrum of underdoped  $\text{YBa}_2\text{Cu}_3\text{O}_{6.6}$  (YBCO) is measured below  $T_c = 59\text{K}$  in parallel magnetic fields  $H//\text{CuO}_2$  up to 7 T. Upon application of a parallel field, a new peak appears at finite frequency in the optical conductivity at the expense of suppression of  $c$ -axis condensate weight. We conclude that the dramatic change originates from different Josephson coupling strengths between bilayers with and without Josephson vortices. We find that the  $400\text{cm}^{-1}$  broad conductivity peak in YBCO gains the spectral weight under parallel magnetic field; this indicates that the condensate weight at  $\omega = 0$  is distributed to the intra-bilayer mode as well as to the new optical Josephson mode.

PACS numbers: 74.25.Gz, 74.72.Bk, 74.50.+r

Josephson plasma oscillation, which generally appears in the  $E//c$  optical response of high  $T_c$  cuprates is a direct consequence of the two-dimensionality of their superconductivity [1, 2, 3, 4]. Depending on the anisotropy parameter  $\gamma = \lambda_c/\lambda_{ab}$ , the Josephson plasma frequency ranges from the microwave ( $\gamma \sim 300 - 1000$  for  $\text{Bi}_2\text{Sr}_2\text{CaCu}_2\text{O}_{8+\delta}$  (Bi-2212) [5, 6, 7]) to the far infrared frequency ( $\gamma \sim 50$  for underdoped YBCO [8, 9, 10, 11, 12] and  $\text{La}_{2-x}\text{Sr}_x\text{CuO}_4$  (LSCO) [1, 13]). The optical/microwave response originates from the restoration of coherent transport due to the tunneling of superconducting carriers between the  $\text{CuO}_2$  layers. The tunneling current, which is driven by the phase-shift between the  $\text{CuO}_2$  layers, is most directly perturbed by the magnetic field applied parallel to the layers; the interplay between parallel field and Josephson tunneling has recently become an interesting subject. Since the tunneling current is involved in the screening of the parallel field, vortices have a large size of  $\sim \gamma s$  within the layers, whereas in the  $c$ -axis direction, they are squeezed to the separation  $s$  of the superconducting layers. This very anisotropic vortex in the parallel field is called a Josephson vortex.

In Bi-2212, there have been microwave resonance measurements under parallel applied magnetic fields [14, 15, 16], and resonance peaks have been observed in microwave absorption spectra. However, in the microwave study, it is not possible to discuss the origin of the observed modes quantitatively. In this Letter, we report a dramatic change of the Josephson plasma mode and an emergence of new modes under parallel fields in underdoped YBCO, where relatively small anisotropy  $\gamma \sim 50$  brings Josephson resonance frequencies up to the far infrared regime. The technique of optical reflectivity was

employed which enabled us to investigate both the resonance energies of longitudinal and transverse modes and their oscillator strengths, necessary for a quantitative discussion of the sum rule.

Another key issue of the  $c$ -axis response of YBCO is the effect of the bi-layer structure. Observations of a broad peak at  $\sim 400\text{cm}^{-1}$  in the optical conductivity which appears below the pseudo-gap temperature have been made by several groups [8, 9, 10, 11, 12]. This “ $400\text{cm}^{-1}$ ” peak has been interpreted as the out-of-phase coupling of the two types of Josephson junctions in YBCO, which correspond to the intra- and the inter-bilayer coupling [17, 18]. Similar observations of this “2nd Josephson plasma mode” have been made in Bi-2212 [24] with the same double pyramid structure as YBCO and  $T^*$ -type compounds, such as  $\text{SmLa}_{1-x}\text{Sr}_x\text{CuO}_4$  [19, 20, 21], which also has two types of insulating layers. Since Josephson vortices penetrate more easily into junctions with weaker Josephson coupling, the applied field is expected to primarily modulate the inter-bilayer coupling in YBCO. It is also interesting to explore the effect of parallel field on the  $400\text{cm}^{-1}$  mode. If there were any effect, it would be direct evidence that superconductivity is involved in the formation of this mode.

The specimen we measured is a  $\text{YBa}_2\text{Cu}_3\text{O}_{6.6}$  single crystal grown by the pulling method [22]. A large crystal ( $10 \times 10 \times 10 \text{ mm}^3$ ) was cut along the  $a \times c$ -plane, post annealed in 1atm  $\text{O}_2$  gas at  $750^\circ\text{C}$  in order to ensure the oxygen content, and then quenched to the room temperature. Magnetic susceptibility (not shown) exhibits a sharp superconducting transition at  $T_c = 59\text{K}$ , with the transition width of less than 2K. The crystal was polished using  $\text{Al}_2\text{O}_3$  powders, and varnished on a sample holder with two  $\phi 6 \text{ mm}$  holes, together with a gold coated glass mirror. We employed a Fourier-transform infrared spectrometer IFS-113v (Bruker) which is equipped with a superconducting magnet SpectroMag (Oxford). We performed calibration measurements in a regular cryostat in

---

\*Electronic address: kojima@lyra.t.u-tokyo.ac.jp

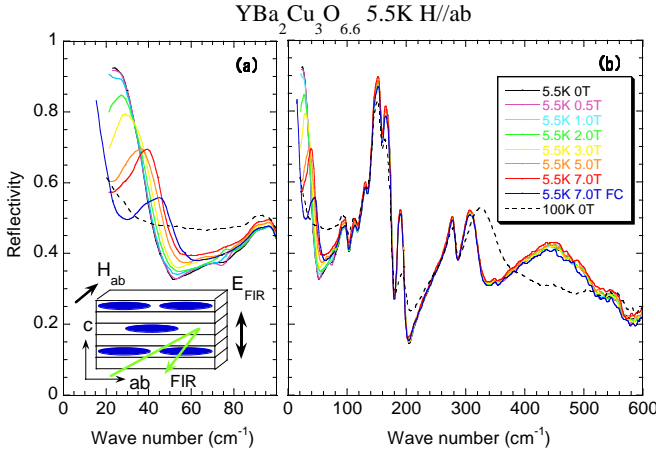


FIG. 1:  $c$ -axis reflectivity of YBCO, under an applied magnetic field  $H//ab$ -plane. All the data shown are taken after zero-field cooling, except the data labeled 7T FC (field cooling).

zero-field. The result agreed with that measured in the magnet. Small misalignments of the magnetic field with respect to the  $\text{CuO}_2$  plane direction do not have serious effects on the result, as the anisotropy is much smaller than that of Bi-2212.

In Figs.1(a) and 1(b), we show the  $c$ -axis optical reflectivity spectra of YBCO at 5.5K and various fields. At zero magnetic field, the Josephson plasma edge is located at  $\sim 45\text{cm}^{-1}$  and a broad bump at  $\sim 400\text{cm}^{-1}$  is observed as has been previously reported [8, 9, 10, 11, 12]. When a parallel magnetic field ( $H_{ab} \geq 1$  Tesla) is applied after the sample has been cooled to 5.5K in zero-field (zero-field cooling: ZFC), the reflectivity edge shifts to higher energy, but simultaneously the reflectivity in the low energy side rapidly decreases, forming a peak. This result demonstrates a surprising sensitivity to the parallel magnetic field. By contrast, a slight and monotonic low energy shift is observed for fields applied perpendicular to the planes (not shown). Fig.1 also shows the data taken after field-cooling at 7T (labeled as “7.0T FC”). In this field-cooling situation, the reflectivity increases below  $\sim 25\text{cm}^{-1}$  forming an additional edge, and the location of the higher energy peak and edge structure is different from that at 7T(ZFC). The spectral difference between FC and ZFC indicates that the observed spectral change is related to the pinning of Josephson vortices.

To make a quantitative analysis of the data, we employed the Kramers-Kronig analysis of the reflectivity, and calculated the optical conductivity  $\sigma(\omega) = \omega \text{Im}(\epsilon)/4\pi$  and the energy loss function  $\text{Im}(-1/\epsilon)$ . The results are shown in Figs.2(a)-(c). A remarkable change in the spectrum is the appearance of a peak in the optical conductivity, labeled as “ $\sigma$ ” in Fig.2(a), which shifts to higher energies with increasing field. The peak intensity, on the other hand, does not depend much on the field strength. The  $\sigma$ -mode obtains appreciable intensity already at  $H_{ab} = 2\text{T}$  (probably at an even lower field in

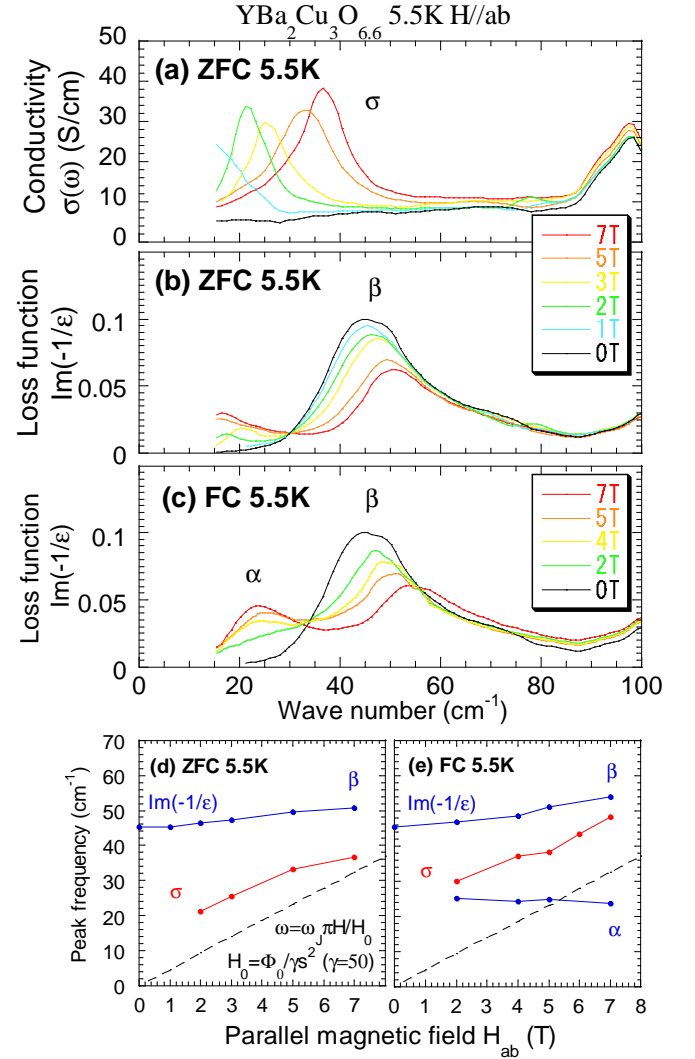


FIG. 2: Optical conductivity (a) and energy loss function (b) at 5.5K after zero-field cooling. (c) Energy loss function at 5.5K after field cooling. Measured peak position of (d) ZFC and (e) FC. The dashed line in (d) and (e) is a theoretical prediction for the high-field limit based on Ref. [27].

view of the data at 1T in Fig.2(a)), which suggests an abrupt growth of intensity upon application of a parallel field. In Figs.2(b) and 2(c), the energy-loss functions which generally measure longitudinal modes are compared for zero-field cooling (ZFC) and field-cooling (FC). In ZFC [Fig.2(b)], there is only one peak observed in our experimental window ( $\omega > 15\text{cm}^{-1}$ ). In FC [Fig.2(c)], there are two peaks emerge within our window. The new longitudinal mode (labeled “ $\alpha$ ”) increases its intensity with  $H_{ab}$ . The original longitudinal mode (labeled “ $\beta$ ”, corresponding to the Josephson plasma mode at  $H_{ab} = 0$ ) decreases in intensity, showing that the spectral weight transferred from  $\beta$ - to  $\alpha$ -mode. This happens also for ZFC, though the  $\alpha$ -peak is not seen above  $15\text{cm}^{-1}$ . The energy positions of the peaks are plotted in Figs.2(d) and 2(e) as a function of  $H_{ab}$ . The peak energy of the  $\beta$ -mode

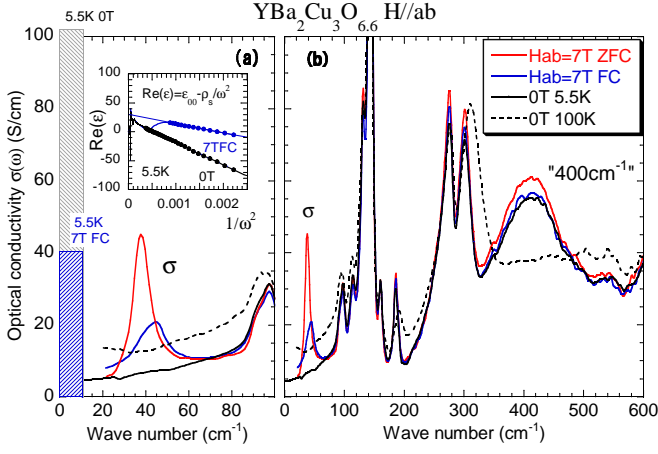


FIG. 3: (a)  $c$ -axis optical conductivity of YBCO, under a parallel field  $H_{ab}$ . The rectangles indicate the weight of low-energy condensate as derived from fitting to the function  $\text{Re}(\epsilon) \approx \epsilon_\infty - \rho_s/\omega^2$  shown in the inset for 0T and 7T(FC) at 5.5K. The filled circles in the inset indicate the data points used for the fitting. (b) Optical conductivity on a wider scale.

shifts upward, whereas the peak energy of the  $\alpha$ -mode decreases slightly with  $H_{ab}$ .

Existence of longitudinal  $\alpha$ -mode, or equivalently, the reflectivity edge below the peak energy, indicates that there is another transverse mode at  $\omega_{\sigma'} < 15 \text{ cm}^{-1}$ . This  $\sigma'$ -mode may be either an  $\omega = 0$  superconducting condensate or a dissipative mode at finite energy. We estimated the spectral weight of this  $\sigma'$ -mode ( $\rho_s$ ) by analyzing the low-energy asymptotic behavior of the dielectric function  $\text{Re}(\epsilon) \approx \epsilon_\infty - \rho_s/\omega^2$  (see inset of Fig.3(a)). This analysis is exact for superconducting condensate, but may have  $\sim \pm 30\%$  error in the spectral weight if  $\omega_{\sigma'}$  is finite. For  $H_{ab} = 0$   $\rho_s$  is a genuine  $c$ -axis condensate weight, and estimated to be  $\rho_s = 4.0(1) \times 10^4 \text{ cm}^{-2}$ . For  $H_{ab} = 7\text{T(FC)}$ , there remains a weight of  $1.5(4) \times 10^4 \text{ cm}^{-2}$  at low energy which locates either at  $\omega = 0$  or at a finite energy  $\omega_{\sigma'}$ . The low energy condensate weights are shown in Fig.3(a) as the height of the rectangles with a width of  $10 \text{ cm}^{-1}$ . For measurements at 7T(ZFC),  $1/\omega^2$  behavior in  $\text{Re}(\epsilon)$  is no longer seen, which suggests that the low- $\omega$  weight is very small.

Optical conductivity over wider energy range is also shown in Fig.3(b). It is clear that the conductivity peak at  $400 \text{ cm}^{-1}$  gains intensity under magnetic fields, especially at 7T(ZFC). The integrated intensity of the  $\sigma$ -peak and the increase in the  $400 \text{ cm}^{-1}$  peak intensity yield  $S(\omega_\sigma) = 1.8(1) \times 10^4 \text{ cm}^{-2}$  and  $\Delta S(\omega_T) = 2.2(2) \times 10^4 \text{ cm}^{-2}$  respectively at 7T(ZFC), which completely exhausts the weight of superconducting condensate at zero-field. On the other hand, at 7T(FC),  $S(\omega_\sigma) = 1.1(1) \times 10^4 \text{ cm}^{-2}$  and  $\Delta S(\omega_T) = 0.5(2) \times 10^4 \text{ cm}^{-2}$ . The sum explains 60-70% of the missing  $\rho_s$  ( $\sim 2.5(4) \times 10^4 \text{ cm}^{-2}$ ) transferred to the  $\sigma$ -mode and the  $400 \text{ cm}^{-1}$  peak. Substantial weight remains in the  $\sigma'$ -mode, which is also evidenced by the evolution of the  $\alpha$ -peak in  $\text{Im}(-1/\epsilon)$  with

increasing  $H_{ab}$  seen in Fig. 2(c). The sum rule analysis gives evidence for spectral-weight transfer from the superconducting condensate to the other two or three finite- $\omega$  transverse modes, enforced by parallel fields or by modulation of the inter-/intra-bilayer coupling.

Now we discuss the origin of the  $\sigma$ -mode. It is proposed that Josephson vortex lattice has a quantized  $c$ -axis lattice parameter ( $= N \times c$ ), whereas its in-plane lattice parameter is tunable to match the external field [25]. In this situation, the inter-bilayer coupling is expected to be modulated, differentiating the Josephson coupling strength between bilayers with and without Josephson vortices, giving rise to a transverse (optical) Josephson plasma mode at finite  $\omega$ . For underdoped YBCO, the anisotropy parameter  $\gamma \sim 50$  scales the characteristic field  $H_0 = \Phi_0/\gamma s^2$  to  $\approx 30\text{T}$  [25, 26]. Calculations of free-energies show that Josephson vortices exist in one out of every two or more layers when  $H_{ab} \lesssim H^* = H_0/3 \approx 10\text{T}$  [25, 26], which very nearly matches our experimental conditions. A phenomenological model which describes the optical response of a Josephson junction array with more than two kinds of insulating layers has been proposed by van der Marel *et al.* [23] which is called as “multi-layer model”. This model has been employed for the analysis of  $c$ -axis optical response of bi-layer compounds in zero-field (YBCO [17, 18] and Bi-2212 [24]) and  $T^*$  materials [19, 20, 21] where two kinds of Josephson couplings are expected due to the crystal structure. We model YBCO in parallel magnetic fields by a simplified multi-layer model which takes into account only the low energy modes in the energy range ( $\omega < 80 \text{ cm}^{-1}$ ) where optical phonons are absent. We assume that the possible  $\sigma'$ -mode is located at  $\omega = 0$ :

$$\frac{\epsilon(\omega)}{\epsilon_\infty} = \frac{(\omega^2 - \omega_\alpha^2)(\omega^2 - \omega_\beta^2)}{\omega^2(\omega^2 - \omega_\sigma^2)} \quad (1)$$

After a simple calculation, the spectral weight of the transverse modes  $S(\omega_\sigma)$  and  $\rho_s$  are given by a function of the energies of these resonance modes. At  $H_{ab} = 7\text{T(FC)}$ , the estimate is straightforward, since all the relevant resonance frequencies are observed. They are  $\omega_\alpha = 23.6 \text{ cm}^{-1}$ ,  $\omega_\sigma = 44.4 \text{ cm}^{-1}$  and  $\omega_\beta = 54.0 \text{ cm}^{-1}$ . Using these frequencies and the dielectric constant  $\epsilon_\infty = 21$ , the calculation gives  $S(\omega_\sigma) = 1.4 \times 10^4 \text{ cm}^{-2}$  and  $\rho_s = 1.7 \times 10^4 \text{ cm}^{-2}$ , in reasonable agreement with the observed  $\sigma$ -peak intensity  $S(\omega_\sigma) = 1.1(1) \times 10^4 \text{ cm}^{-2}$  and the  $\sigma'$ -peak intensity (or superconducting condensate)  $\rho_s = 1.5(4) \times 10^4 \text{ cm}^{-2}$ . At 7T(ZFC), the location of the  $\alpha$ -peak is uncertain which makes the estimate somewhat ambiguous. Also in this case, the observed  $\sigma$ -peak intensity  $1.8(1) \times 10^4 \text{ cm}^{-2}$  is consistent with a rough estimate of  $\approx 2 \times 10^4 \text{ cm}^{-2}$ . These agreements supports the hypothesis that the  $\sigma$ -mode originates from the periodic modulation of inter-bilayer Josephson coupling strength due to the Josephson vortices.

A theoretical investigation of Josephson plasma in parallel field was performed by Bulaevskii *et al.* under the ideal condition of absence of pinning to the Joseph-

son vortices [27]. They found two strong resonance modes: one corresponding to “vortex sliding mode”, and the other arising from the Josephson plasma dispersion folded to the zone center by the formation of a vortex superlattice [27]. The spectral weight is transferred from the latter to the former with  $H_{ab}$ . In real materials, the vortex sliding mode is expected to be influenced by pinning of the Josephson vortices; the  $\sigma'$ -mode (or the associated longitudinal  $\alpha$ -mode) in YBCO depends on the field-cycle and may be assigned to the pinned sliding mode of Josephson vortices. The energy of the “folded Josephson plasma mode” calculated in high field limit [27], presents a linear field dependence as shown in Figs.2(d) and 2(e) by the dashed line. It appears that the energy of the  $\sigma$ -mode (or the associated  $\beta$ -mode) in YBCO tends to approach this line at higher fields. In fact, the spectral weight transfer between  $\alpha$ - and  $\beta$ -mode shown in Figs. 2(b) and 2(c) is consistent with the theoretical result [27]. Recent microwave measurement of Bi-2212 under parallel field has revealed two resonance modes [16]. In the light of the present results for YBCO, it is likely that the higher energy mode corresponds to the  $\beta$ - (or  $\sigma$ -) mode, and the low-energy mode to the  $\alpha$ -mode (or  $\sigma'$ -mode).

The reason why the transverse  $\sigma$ - and  $400\text{cm}^{-1}$  modes are considerably more enhanced in ZFC than in FC might be related to the pinning of Josephson vortices. As the alternating stack of insulating layers with and without Josephson vortices is most likely the source of the  $\sigma$ -mode, disorder in stacking would reduce the  $\sigma$ -mode intensity. This seems to be the case with the  $\sigma$ -mode for FC, since random distribution of pinning centers tends to

make the stacking of Josephson vortices more disordered. In a  $T^*$  cuprate  $\text{Nd}_{2-x-y}\text{Sr}_x\text{Ce}_y\text{CuO}_4$ , reduced intensity of the transverse Josephson plasma mode has been interpreted as the result of disorder in the crystalline structure [20].

In LSCO, no new transverse  $\sigma$ -mode under parallel field is seen [28, 29, 30], although the anisotropy parameter  $\gamma$  is in the same order of magnitude with underdoped YBCO. Only a low- $\omega$  shift of the Josephson plasma edge is observed with increasing parallel field, suggesting that the Josephson vortices would be highly disordered seemingly due to fluctuations of stripe order in LSCO.

In conclusion, we have demonstrated a remarkable effect of parallel magnetic field on the  $c$ -axis Josephson plasma mode in underdoped YBCO. Parallel magnetic field modulates the inter-bilayer Josephson coupling strength along the  $c$ -axis due to the presence of inequivalent insulating layers with and without Josephson vortices. As a result, one optical (transverse) mode appears, corresponding to the anti-phase Josephson current oscillations between two inequivalent junctions. Another consequence of the modulation of the inter-bilayer coupling and/or suppression of inter-bilayer coherent pair hopping is the enhanced intensity of the  $400\text{cm}^{-1}$  mode. This gives evidence that this mode is a marker of superconducting Josephson coupling within a bilayer.

The authors would like to thank Prof. M. Tachiki, Drs. Y. Ando, M. Machida, I. Kakeya and T. Kakeshita for stimulating discussions. The research in this paper has been financially supported by NEDO International Joint Research Grant and by COE & Grant-in-aid for Scientific Research from Monbusho.

- 
- [1] K. Tamasaku, Y. Nakamura and S. Uchida, *Phys. Rev. Lett.* **69**, 1455 (1992).
  - [2] M. Tachiki, T. Koyama and S. Takahashi, *Phys. Rev. B* **50**, 7065 (1994); T. Koyama and M. Tachiki, *Phys. Rev. B* **54**, 16183 (1996).
  - [3] L.N. Bulaevskii, V.L. Pokrovsky, M.P. Maley, *Phys. Rev. Lett.* **76**, 1719 (1996); L.N. Bulaevskii *et al.*, *Phys. Rev. B* **54**, 7521 (1996).
  - [4] Y. Ohashi and S. Takada, *J. Phys. Soc. Jpn.* **66**, 2437 (1997); *J. Phys. Soc. Jpn.* **67**, 551 (1998).
  - [5] Y. Matsuda *et al.*, *Phys. Rev. Lett.* **75**, 4512 (1995); *Phys. Rev. Lett.* **78**, 1972 (1997).
  - [6] K. Kadowaki *et al.*, *Physica C* **293**, 130 (1997); *Physica B* **239**, 123 (1997); *Phys. Rev. B* **56**, 5617 (1997); I. Kakeya *et al.*, *Phys. Rev. B* **57**, 3108 (1998).
  - [7] T. Motohashi, *et al.*, *Phys. Rev. B* **61**, R9269 (2000).
  - [8] C.C. Homes *et al.*, *Phys. Rev. Lett.* **71**, 1645 (1993).
  - [9] R. Hauff *et al.*, *Phys. Rev. Lett.* **77**, 4620 (1996).
  - [10] S. Tajima *et al.*, *Phys. Rev. B* **55**, 6051 (1997).
  - [11] C. Bernhard *et al.*, *Phys. Rev. B* **61**, 618 (2000).
  - [12] Y. Fukuzumi, K. Mizuhashi and S. Uchida, *Phys. Rev. B* **61**, 627 (2000).
  - [13] S. Uchida, K. Tamasaku and S. Tajima, *Phys. Rev. B* **53**, 14558 (1996).
  - [14] Y. Matsuda *et al.*, *Phys. Rev. B* **55**, R8685 (1997).
  - [15] K. Kadowaki, T. Wada and I. Kakeya, *Physica C* **362** 71 (2001).
  - [16] I. Kakeya, *et al.*, cond-mat/0111094.
  - [17] D. Munzar, *et al.*, *Solid State Commun.* **112**, 365 (1999); *Phys. Rev. B* **64**, 024523 (2001).
  - [18] M. Grüninger *et al.*, *Phys. Rev. Lett.* **84**, 1575 (2000).
  - [19] H. Shibata, *Phys. Rev. Lett.* **86**, 2122 (2001).
  - [20] T. Kakeshita *et al.*, *Phys. Rev. Lett.* **86**, 4140 (2001).
  - [21] Diana Dulic, *et al.*, *Phys. Rev. Lett.* **86**, 4144 (2001).
  - [22] Y. Shiohara and A. Endo, *Mater. Sci. Eng.* **R19**, 1 (1997), and references therein.
  - [23] D. van der Marel and A.A. Tsvetkov, *Czech. J. Phys.* **46**, 3165 (1996); *Phys. Rev. B* **64**, 024530 (2001).
  - [24] V. Zelezny *et al.*, *Phys. Rev. B* **63**, 60502 (2001).
  - [25] L. Bulaevskii, and John R. Clem *Phys. Rev. B* **44**, 10234 (1991).
  - [26] M. Ichioka, *Phys. Rev. B* **51**, 9423 (1995).
  - [27] L.N. Bulaevskii *et al.*, *Phys. Rev. B* **55**, 8482 (1997).
  - [28] S. Kimura, *J. Phys. Soc. Jpn.* **65** Suppl. B, 109 (1996).
  - [29] A.M. Gerrits, *et al.*, *Phys. Rev. B* **51**, 12049 (1995).
  - [30] P.J.M. van Bentum, *et al.*, *Physica C* **293**, 136 (1997).